Resonant Two-Photon Ionization Spectroscopy of Styrene (Methanol)$_n$ Clusters, $n = 1-9$

H. Mahmoud, I. N. Germanenko, Y. Ibrahim, and M. S. El-Shall*

Department of Chemistry, Virginia Commonwealth University, Richmond, Virginia 23284-2006

Received: February 10, 2003

Well-resolved spectra of styrene−methanol binary clusters SM_n, with $n = 1-9$, have been obtained by the (one-color) resonant two-photon ionization technique using the 0_0^0 resonance of styrene. The spectra reveal a rapid increase in complexity with the number of methanol molecules in the cluster, associated with van der Waals modes and isomeric forms. Two distinct isomers are identified for each of the clusters studied with the exception of SM_4 and SM_8. The progressive addition of methanol molecules to the SM complex leads to the formation of stable cyclic and branched cyclic methanol subclusters within the SM_n clusters. The spectral shift of the cluster origin reflects the nature of the intermolecular interactions within the binary cluster. Blue shifts are observed for the SM, SM_2, and SM_3 clusters and are consistent with hydrogen bonding interactions between the OH groups and the styrene π-system. A remarkable switch in the spectral shift from blue to red is observed at the SM_4 cluster and is consistent with the ring structure of the methanol tetramer. Evidence is provided for intracluster dissociative proton-transfer reactions within the $S_2M_n^+$ ($n > 2$) clusters that generate protonated methanol clusters. These reactions may explain the strong inhibition effects exerted by small concentrations of methanol on the cationic polymerization of styrene.

I. Introduction

The study of molecular clusters of varying sizes and compositions constitutes an active and fascinating area of research. These clusters provide microscopic models for a molecular level understanding of a variety of important condensed phase phenomena such as solvation, phase transitions, nucleation, microphase separation, polymerization reactions, protein folding, and molecular recognition.[1−9]

Binary clusters composed of a nonpolar aromatic center and polar or hydrogen-bonded solvent molecules represent an important class of molecular clusters. Several examples of these clusters have been investigated in recent years using combinations of spectroscopic and theoretical techniques.[5−9] The majority of the work has been focused on benzene in the presence of various polar and hydrogen bonding molecules.[5−19] For example, extensive studies have been conducted on the benzene−water (BW_n) and benzene−methanol (BM_n) clusters using spectroscopic techniques such as resonant two-photon ionization (R2PI), hole burning, and resonant ion-dip infrared spectroscopy.[9−16,20,21] These studies have established several characteristic features of the intermolecular interactions between aromatic π-systems and hydrogen bonded solvent molecules. Among these features are (a) the blue spectral shifts in small clusters, which seem to increase with increasing hydrogen bonding ability of the solvent molecules, (b) the gradual switch to red shifts in larger clusters, (c) the tendency of the solvent molecules to form a hydrogen bonding network in a one-sided structural type with the benzene ring, and (d) the very efficient fragmentation of the photoionized clusters, which has been interpreted as a direct consequence of the hydrogen bonding to the benzene ring.[9] For a complete understanding of these systems, it is desirable to study other aromatic systems, including those in which an additional π-interaction site is available.

Styrene is the simplest molecule that contains an unsaturated group covalently linked to an aromatic ring, and therefore represents a model system for studying the interactions between different π-systems with H-bonded molecules such as water and methanol. The unsaturated side chain provides an additional site for π-interaction with polar molecules that competes with the aromatic ring. These interactions are relevant to a wide variety of chemical, photochemical, and biological processes in several fields such as photoconductivity, light-induced charge and electron-transfer reactions, and polymer chemistry.[1−3,22−24] Styrene polymerization is among the most extensively studied polymerization process and continues to attract interest. The molecule is known to undergo polymerization in bulk monomer or in solution by free radical, cationic, and anionic mechanisms.[25,26] The thermally initiated gas-phase polymerization has been demonstrated and efforts to achieve a molecular level understanding of the various processes taking place during the polymerization continue to increase the potential of designing novel polymeric materials with unusual advanced properties.

In condensed phases, the crucial role played by trace amounts of water and other protic impurities on the mechanism and rate of polymerization in styrene is widely recognized. Under very dry conditions, radiation-induced polymerization of the bulk monomer proceeds rapidly,[26,27] but under "wet" conditions ($[H_2O] > 10^{-3}$ M) polymerization proceeds more slowly.[27] Small amounts of methanol are also known to suppress polymerization and enhance dimerization in styrene.[28] The study of styrene−water (SW_n) and styrene−methanol (SM_n) clusters can provide information on the interactions involved in these systems and a greater molecular level understanding of the retardation and inhibition effects of water and methanol on polymerization in styrene. The addition of the first few solvent molecules to the styrene molecule provides information on the preferred solvent sites and their relative strengths. The addition of further molecules yields information on solvent cooperative effects, coordination, and formation of solvent shells around the reactive monomer species.

The particular system of interest in the present study consists of a single styrene molecule (S) and several methanol molecules,

10.1021/jp0301756 CCC: $25.00
Published on Web 07/12/2003

i.e., SM_n with $n = 1-9$. Like water, methanol can participate in relatively weak hydrogen bonding to the π-system of styrene. However, the presence of the methyl group provides a favorable site for hydrophobic interaction, making methanol, the smallest alcohol, subject to both hydrogen bonding and hydrophobic forces.[2,22] Methanol differs substantially from water in its tendency to form chainlike polymeric units in the liquid phase similar to those found in the solid state.[29,30] Methanol clusters containing a styrene molecule raise the interesting question of whether the structural features observed in the neat clusters would be retained in the presence of styrene, and whether the trend in the spectral shift of the SM_n clusters could provide information on the structures of the clusters. If hydrogen bonding among the methanol molecules is stronger than the dipole−induced dipole interaction between methanol and styrene, then little change is to be expected in the gross structural features of methanol clusters when styrene is present. The examination of this and other related questions is the subject of the present work, which presents the results of ultraviolet spectroscopy of the SM_n clusters for $n = 1-9$ using the resonant two-photon ionization (R2PI) technique. In the companion paper we investigate the structures of the clusters using pair-potential (OPLS, optimized Potential for Liquid Simulation) calculations.[31] The combination of the R2PI spectra and the theoretical calculations provides a reasonably compelling picture of the interactions involved in these systems. Detailed knowledge of these interactions is a prerequisite for a molecular level understanding of the retardation and inhibition effects of methanol on the cationic polymerization of styrene.

II. Experimental Section

Binary SM_n clusters are generated by pulsed adiabatic expansion in a supersonic cluster beam apparatus.[17−19] The essential elements of the apparatus are jet and beam chambers coupled to a time-of-flight mass spectrometer. The binary clusters are formed in a He-seeded jet expansion and probed as a skimmed cluster beam in a collision-free high vacuum chamber with a delay between synthesis and probe (i.e., the neutral beam flight time) on the order of 1 ms. During operation, a vapor mixture of styrene−methanol is prepared by flowing He (ultrahigh purity, Spectra Gases 99.999%) over the two separate temperature-controlled liquids and mixing these flows with the main flow of He. The vapor mixture at a pressure of 8 atm is expanded through a conical nozzle (100 μm diameter) in pulses of 200−300 μs duration at repetition rates of 5−8 Hz. The jet is skimmed and passed into a high vacuum chamber, which is maintained at 8×10^{-8} to 2×10^{-7} Torr. The collimated cluster beam passes into the ionization region of the TOF mass spectrometer where it intersects a laser pulse from a frequency-doubled dye laser. The tunable radiation is provided by a dye laser (Lambda Physik FL3002) pumped by an excimer laser (Lambda Physik LPX-101). Coumarin 540A (Exciton) dye laser output passes through a β-BaB_2O_4 crystal to generate a continuously tunable frequency-doubled output of 10^{-8} s pulses. The spatially filtered (using a set of four quartz Pellin-Broca prisms) ultraviolet radiation is adjusted to minimize three photon processes while still providing sufficient ion current (photon power density $\approx 2.5 \times 10^5$ W/cm^2). The cluster ions formed by R2PI are electrostatically accelerated in a two-stage acceleration region (300−400 V/cm) perpendicular to the direction of the neutral beam, and then travel a field-free region (170 cm in length) to a two-stage microchannel-plate detector. Deflection plates are used to compensate for the ion beam velocity in the direction of the neutral cluster beam. The TOF spectrum is recorded by digitizing the amplified current output of the detector with a 500 MHz digitizer (LeCroy 9350A) and averaged over 200 pulses.

The spectra displayed in Figures 1−5 are selected from a great number of experiments under a range of conditions, characterized primarily by the concentrations of styrene and methanol vapors in the preexpansion mixture, the seed ratio in He and total pressure. The relative concentrations studied (styrene:methanol:He) range from ($1:1.4 \times 10^2:5.2 \times 10^7$) to ($1:5 \times 10^4:5.2 \times 10^7$). Several concentration studies have been performed to identify the spectral features arising from different cluster series such as the S_2M_n and S_3M_n series. The reported spectra were all obtained with the minimum concentration of styrene vapor in the preexpansion mixture that allowed the observation of mainly the SM_n series (the lowest concentration of styrene corresponded to a sample temperature of −75 °C at which the vapor pressure is roughly 2×10^{-4} Torr). We have performed repeated sets of experiments with different concentrations of methanol in the preexpansion series to control the distribution of the SM_n neutral clusters. For example, the spectra of the SM and SM_2 clusters were confirmed by generating small SM clusters using a trace concentration of methanol vapor (by flowing He over methanol kept at −75 °C corresponding to a vapor pressure of 2.8×10^{-2} Torr). The spectral features that showed dependence on the methanol concentration in the preexpansion mixtures were confirmed to be arising from higher clusters. All the spectral features reported in the paper were reproduced many times under a variety of concentration and laser power conditions.

III. Results and Discussion

A. Styrene Spectroscopy. Several groups have studied the low-lying electronic states of styrene, experimentally and theoretically, over the past thirty years.[32−44] The experimental data indicated that the molecule is planar in both the ground and first electronically excited singlet states. No evidence was obtained for a "perpendicular" orientation of the CH_2 group in the S_1 state. Ab initio structural calculations compatible with the measured rotational constants conclusively established the planarity of the molecule.[37] Recent calculations suggested that the ground state may be slightly bent, whereas the lowest two excited states are strictly planar.[41] At the HF/4-31G level of theory, the ground state was found to have a broad shallow potential as a function of the torsional angle (τ) of the −CH=CH_2 group with a minimum energy at $\tau = 10.5°$.[41] However, it has been always assumed that the small deviation from planarity is due to a computational deficiency.[39−42] The electronic origin band of the $S_0 \rightarrow S_1$ transition of styrene is located at 34 758.79 cm^{-1} and the transition moment is parallel to the long in-plane axis.

Figure 1a displays the R2PI spectra obtained by monitoring the mass channel corresponding to styrene (S) in the 0_0^0 region between 34 700 and 35 000 cm^{-1}. The spectrum shows the 0_0^0 origin and the vibronic bands 41_0^2 and 29_0^1 as well as the cross-sequence bands $41_0^1 42_0^1$ between the ν_{42} and ν_{41} modes (ethylene group torsional rotation and out-of-plane bend, respectively), $41_0^1 42_1^0$ and $41_0^3 42_1^0$. The spectrum is in very good agreement with previous fluorescence excitation and REMPI studies.[34,43,44] The other small features shown in the spectrum of Figure 1a are due to hot bands (29_1^1 and 42_1^1) and some minor features (marked with asterisks) correspond to SM_n clusters that fragment to the S mass channel. These features will be discussed in the next section.

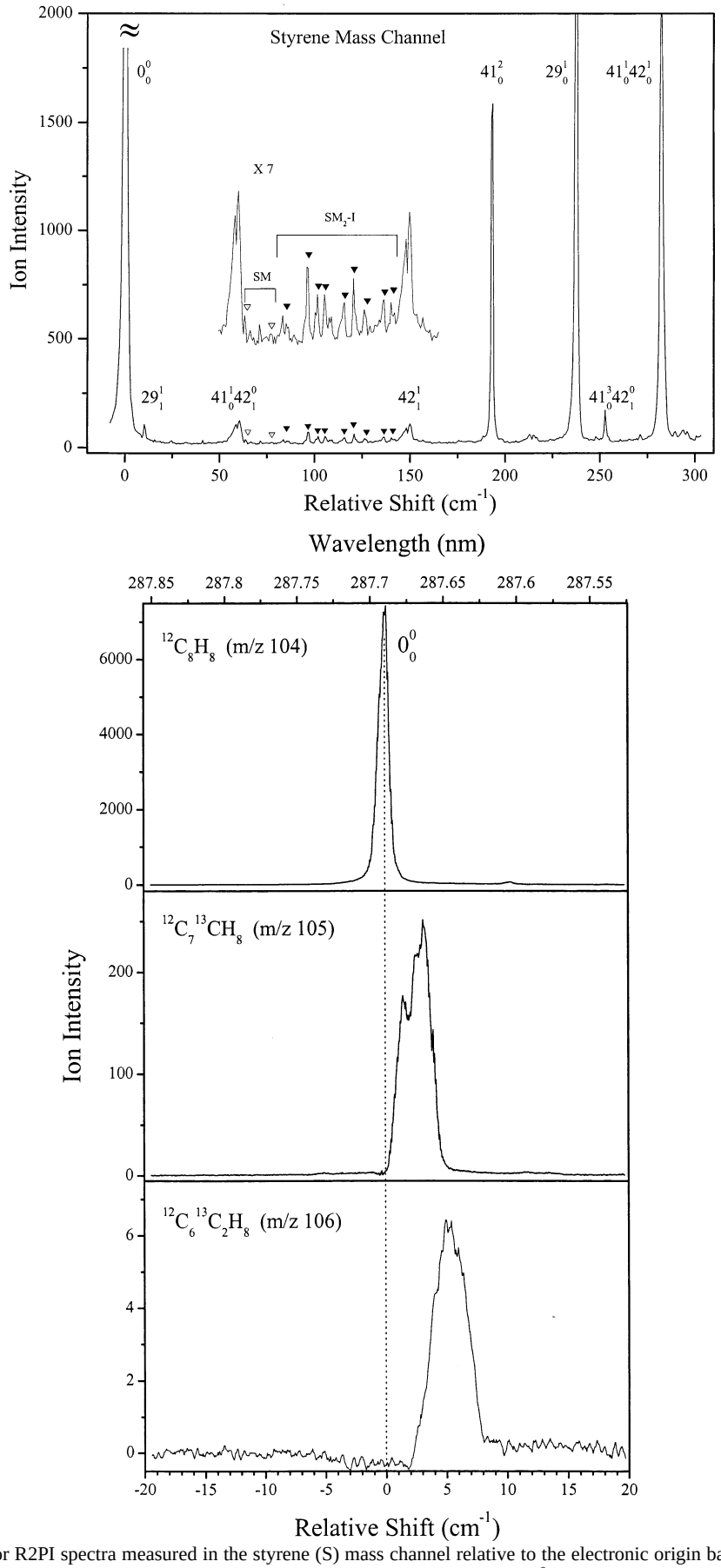

Figure 1. (a, top) One-color R2PI spectra measured in the styrene (S) mass channel relative to the electronic origin band of the $S_1 \leftarrow S_0$ transition of the styrene molecule at 34 758.79 cm^{-1}. (b, bottom) Effect of isotopic substitution on the 0_0^0 band of styrene.

Figure 1b displays the styrene 0_0^0 band obtained by monitoring the mass channels corresponding to C_8H_8, $^{13}CC_7H_8$, and $^{13}C_2C_6H_8$ (zero, one, and two ^{13}C isotopes in C_8H_8, $m/z = 104$, 105, and 106, respectively). The spectra show that the replace-

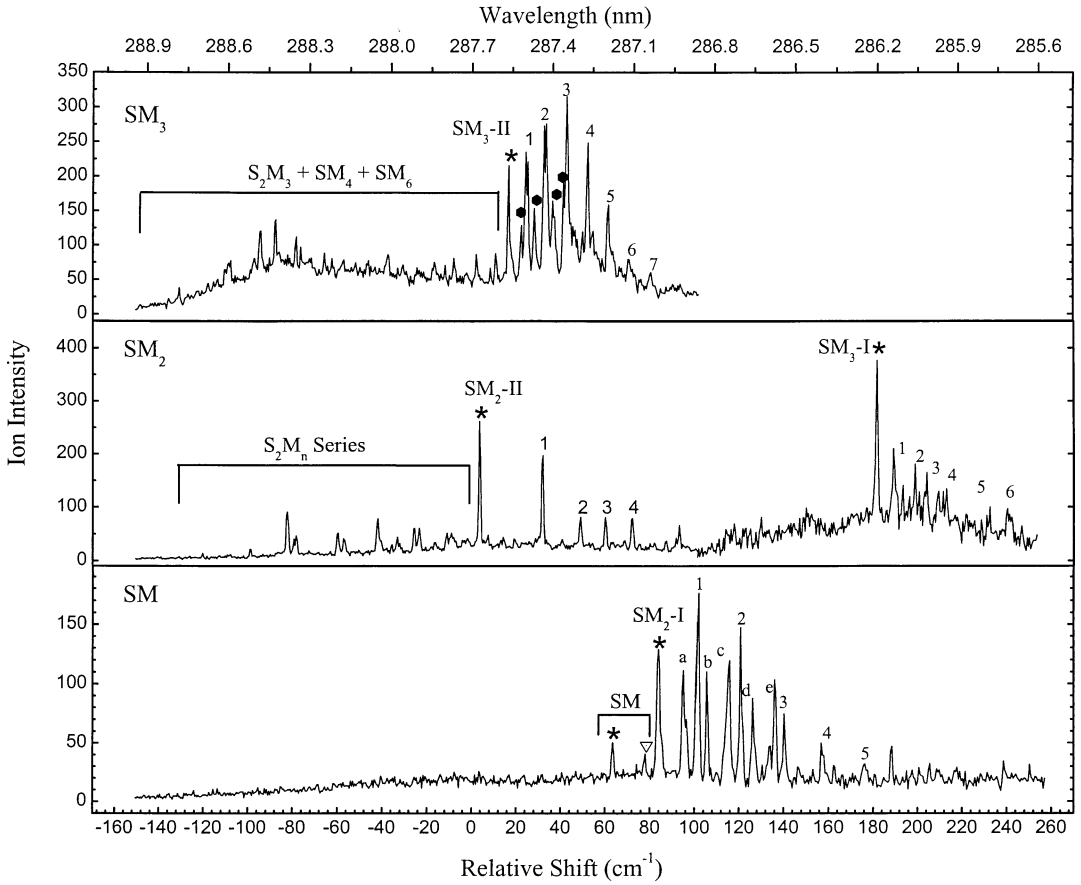

Figure 2. One-color R2PI spectra measured in the styrene (methanol)$_n$ mass channels with $n = 1-3$ [SM, SM_3, and SM_3], relative to the electronic origin band of the $S_1 \leftarrow S_0$ transition of the styrene molecule at 34 758.79 cm^{-1}. The origin of each cluster isomer is marked with an *. The peaks labeled with numbers, letters, or symbols following each cluster's origin represent vdW bands associated with the cluster origin (see Table 1).

ment of one and two ^{12}C with ^{13}C atoms results in small blue shifts of the 0_0^0 band by 2.5 and 5 cm^{-1}, respectively. Similarly, the shift of the 0_0^0 can also be induced by the clustering of atoms or molecules around the styrene molecule.

B. Spectra of Small SM$_n$ Clusters, $n = 1-3$. Figure 2 displays the spectra obtained by monitoring the mass channels corresponding to SM, SM_2, and SM_3 clusters. The SM channel shows several strong features, which appear in the SM_2 channel with very small intensities. The peak at 63.5 cm^{-1} relative to the 0_0^0 of styrene (not present in the SM_2 mass channel) is assigned to the 0_0^0 of the SM complex with a small peak at 78 cm^{-1} assigned to a vdW vibration of the complex. Several other peaks at 95, 106, 116, and 126.5 cm^{-1} from the 0_0^0 of styrene could also be assigned a vdW progression built on the SM origin.

The stronger peak at 83.8 cm^{-1} accompanied by two rich vdW progressions is assigned to one isomer of the SM_2 cluster (SM_2-I). The SM_2-I cluster possesses two long progressions of bands assigned to the excitation of intermolecular vibrational modes. The first progression appears at 102, 121, 140.6, 157, and 176.6 cm^{-1} (corresponding to peaks 1−5, respectively, in the SM channel in Figure 2). The second progression corresponds to peaks a−e shown in the SM channel at frequencies 96, 106, 116, 126.5, and 136 cm^{-1}, respectively. It should be noted that the peaks a−d are relatively broad and they overlap with the vdW progression assigned to the SM cluster. Therefore, it appears that the series of peaks a−e contain contributions from both the vdW progressions of the SM and SM_2 clusters. The appearance of strong vibronic intensities away from the origin of the SM and SM_2-I clusters indicates that Franck−Condon factors do not favor the cluster origin intensity, thus the ground state and excited-state geometries of the SM and SM_2-I isomer are quite different.

The SM_2 mass channel shows three sets of peaks. The small red-shifted peaks, relative to the 0_0^0 of the styrene, are due to higher clusters containing the styrene dimer S_2. These features are found in the mass channels corresponding to S_2M_2 and S_2M_3 clusters at the same frequencies as they appear in the SM_2 channel. The second group consists of a strong peak blue shifted by 3.4 cm^{-1} from the 0_0^0 of styrene. This peak is assigned to a second isomer of the SM_2 cluster (SM_2-II) with a vdW progression at 32, 49, 60, and 72 cm^{-1} (corresponding to peaks 1−4 following the SM_2-II origin in the SM_2 channel in Figure 2). It is interesting that the second isomer SM_2-II does not show significant fragmentation upon photoionization. This suggests that the SM_2-II isomer possesses a distinct structure from that of the SM_2-I isomer, and that this structure does not appear to undergo major changes upon photoionization. The calculated structures of the SM$_n$ clusters are presented and discussed in the companion paper.[31]

The third group of peaks observed in the SM_2 mass channel starts with a sharp peak at 182 cm^{-1} followed by a vdW progression of very low-frequency modes at 189, 199, 204, 213, 232, and 341 cm^{-1} (corresponding to peaks 1−6 following the SM_3-I origin in the SM_2 channel in Figure 2). Some of these peaks appear with very small intensities in the SM_3 mass channel, and may be tentatively assigned to one isomer of the SM_3 cluster (SM_3-I).

The most prominent features in the SM_3 mass channel can be assigned to a second isomer of the SM_3 cluster with a strong

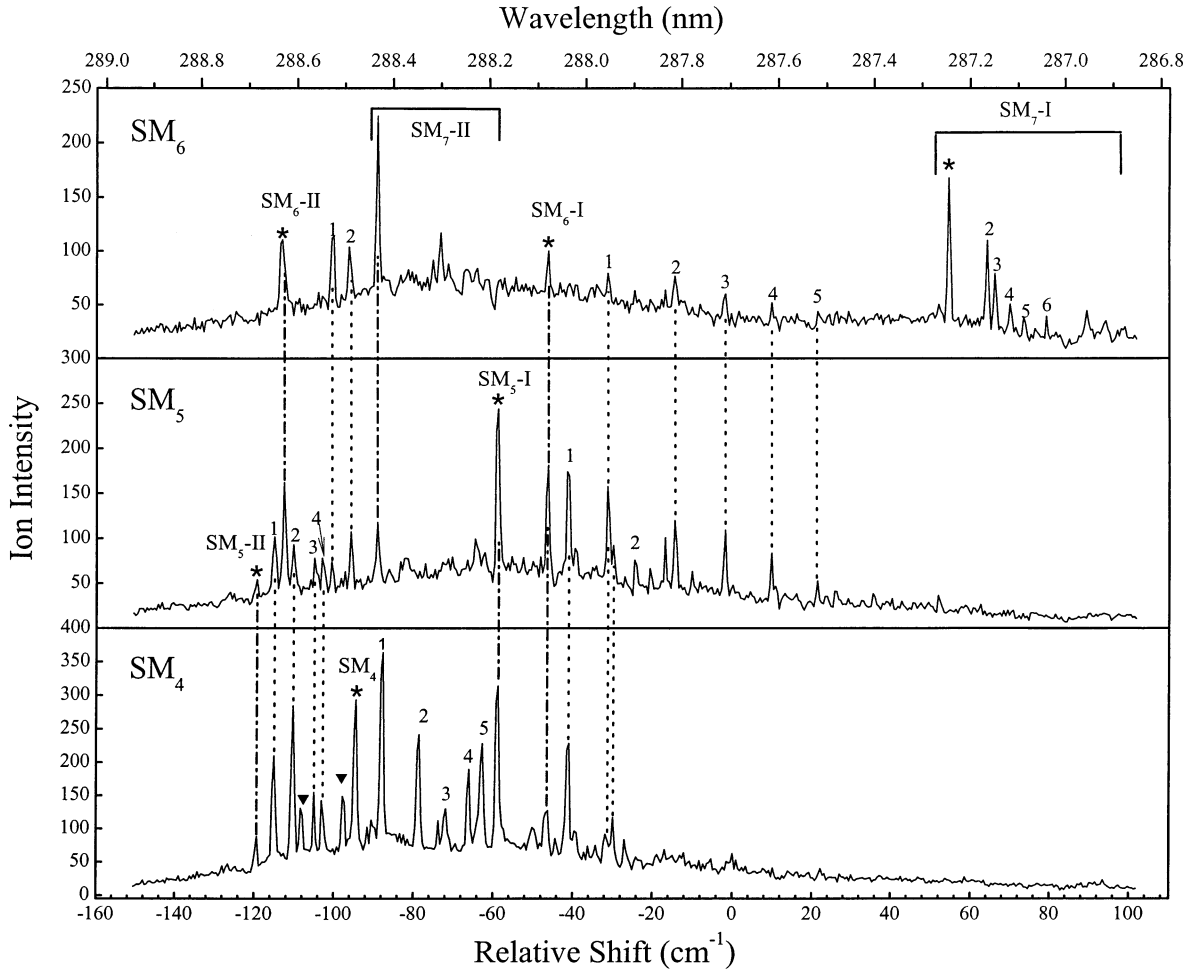

Figure 3. One-color R2PI spectra measured in the styrene (methanol)$_n$ mass channels with $n = 4-6$ [SM_4, SM_5, and SM_6], relative to the electronic origin band of the $S_1 \leftarrow S_0$ transition of the styrene molecule at 34 758.79 cm^{-1}. The origin of each cluster isomer is marked with an *. The peaks labeled with numbers following each cluster's origin represent vdW bands associated with the cluster origin (see Table 1). The two peaks labeled with ▼ at −108 and −98 cm^{-1} from the styrene origin in the SM_4 mass channel are unassigned.

origin peak blue shifted from the styrene origin by 16.5 cm^{-1}. This origin is accompanied by a strong vibronic intensity with a well-defined vdW progression of doublets at 24, 33, 43, 52, 62, 70, and 80 cm^{-1}. In addition, two other weaker peaks appear at 28 and 36 cm^{-1}. Several weaker features to the red of the SM_3-II isomer are due to fragmentation from the SM_4 cluster.

The blue shift observed for the SM cluster (63 cm^{-1}) is consistent with a weak hydrogen bonding interaction between the OH group of methanol and the styrene π-system. For example, benzene complexes with H_2O, CH_3OH, CH_3COOH, HCl and $CHCl_3$ exhibit blue shifts of 52, 44, 152, 125, and 179 cm^{-1}, respectively.[10−14,17] It is interesting to note that the addition of a second methanol molecule to styrene results in a greater blue shift in the SM_2-I cluster (84 cm^{-1}). This is very similar to the benzene (methanol)$_n$ clusters, BM_n, where the spectral shifts of BM and BM_2 clusters relative to the 6_0^1 origin of the isolated benzene molecule are 44 and 80 cm^{-1}, respectively.[14] Also, the spectrum of the SM_2 cluster exhibits several vdW transitions indicating that the 1:2 clusters undergo major changes in geometries upon the electronic excitation of styrene. This is exactly the same trend found in the BM_2 clusters.[14] Furthermore, in both the benzene and styrene systems extensive fragmentation is observed following photoionization of the neutral clusters. The high fragmentation probability of the ionized clusters is consistent with the hydrogen bonding interaction with the π-system in benzene or styrene.

A noticeable difference between the benzene and styrene systems is the assignment of two structural isomers to the SM_2 cluster with quite different spectral shifts (84 and 3.4 cm^{-1} relative to the 0_0^0 transition of styrene). This is in contrast to the BM_2 cluster, where only one isomer was assigned.[14] The interactions between the ethylene group of styrene and the methyl group in methanol are considered to be purely dispersive. This suggests that the SM_2-II isomer may represent a structure that maximizes induced dipole−induced dipole forces between the ethylene group of styrene and the methyl groups of the two methanol molecules. This interaction is known to lead to red spectral shifts, and therefore one expects the SM_2-II isomer to exhibit a significant red shift relative to the SM complex ($\Delta\nu = -60$ cm^{-1}). The dominance of the dispersion interaction and the small π-hydrogen bonding interaction in the SM_2-II isomer is consistent with the low fragmentation probability observed for this isomer following photoionization.

The blue-shifted isomer assigned to the SM_3 cluster (SM_3-I) may have a hydrogen-bonded methanol chain structure H-bonded to the styrene π-system. This structure is compatible with the strong blue shift observed (182 cm^{-1} with respect to the styrene origin). The second isomer (SM_3-II) may reflect a cyclic methanol structure with no hydrogen bonding to styrene because all the OH groups would be used in the formation of the methanol trimer ring. This isomer has a smaller blue shift of 16 cm^{-1}, consistent with the absence of hydrogen bonding

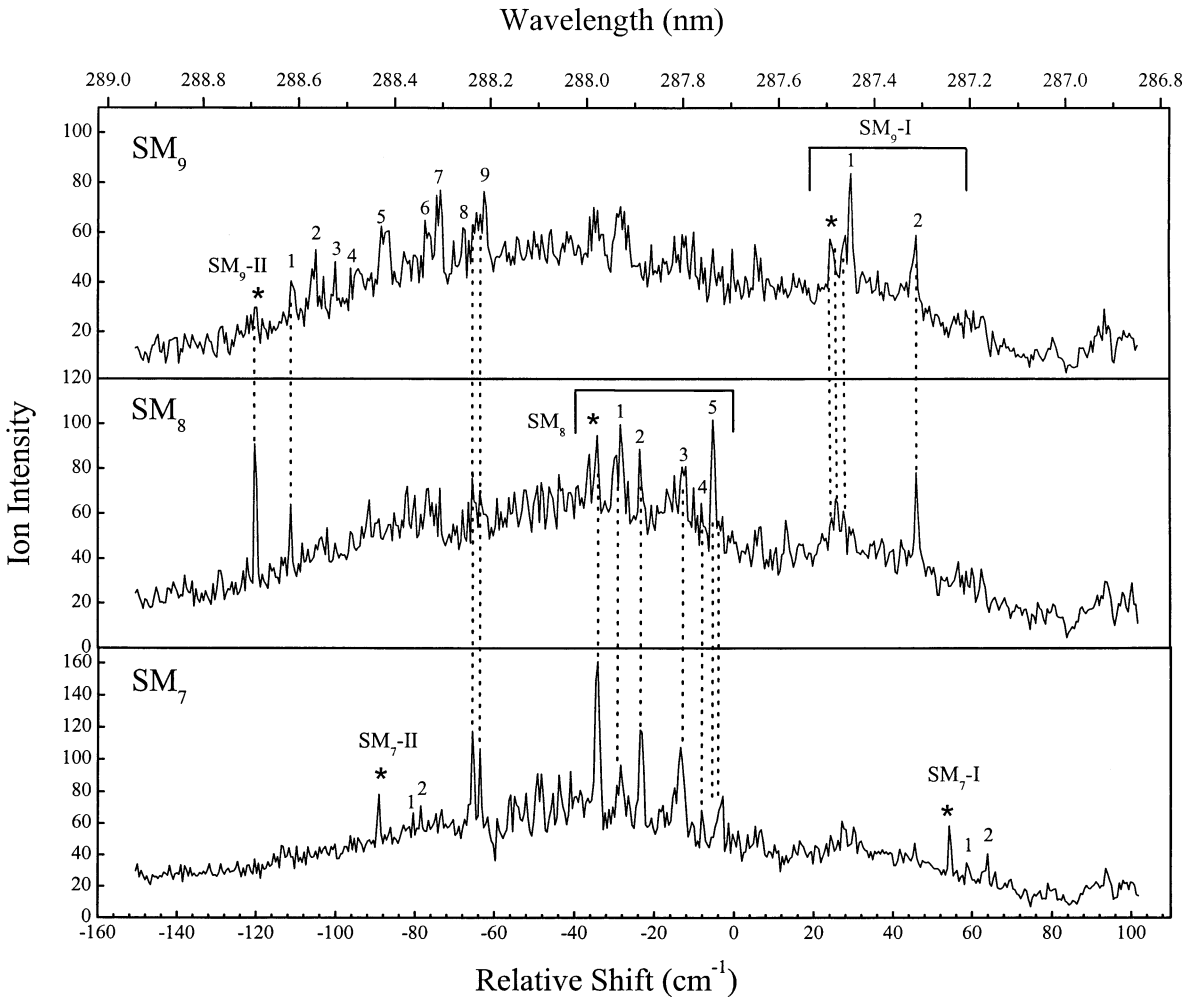

Figure 4. One-color R2PI spectra measured in the styrene (methanol)$_n$ mass channels with $n = 7-9$ [SM_7, SM_8 and SM_9], relative to the electronic origin band of the $S_1 \leftarrow S_0$ transition of the styrene molecule at 34 758.79 cm^{-1}. The origin of each cluster isomer is marked with an *. The peaks labeled with numbers following each cluster's origin represent vdW bands associated with the cluster origin (see Table 1).

interaction to the styrene π-system. The calculated structures of the SM_n clusters, presented and discussed in the companion paper,[31] are consistent with the structural predictions presented here based on the observed spectral shifts and the degree of cluster's fragmentation following ionization.

C. Spectra of SM_n Clusters, $n = 4-6$. The R2PI spectra obtained by monitoring the mass channels corresponding to the SM_4, SM_5, and SM_6 clusters in the region of the styrene 0_0^0 transition are displayed in Figure 3. A remarkable shift in the spectra from blue to red, with respect to the styrene origin, is observed starting at the SM_4 cluster. Also, ion fragmentations from the S^+M_5 and S^+M_6 clusters to the S^+M_4 channel appear to be pronounced because several features belonging to the SM_5 and SM_6 clusters are present in the S^+M_4 mass channel. The strong set of peaks in the -98 to -60 cm^{-1} region are assigned to the SM_4 cluster with the origin assigned to the singlet at -94 cm^{-1}. A vdW progression associated with the cluster origin also appears at -88, -79, -72, -66, and -62 cm^{-1} (corresponding to peaks $1-5$ following the SM_4 origin in the SM_2 channel in Figure 3). The cluster origin and the vdW modes also appear in the SM_3 channel as a result of the ion fragmentation process $S^+M_4 \rightarrow S^+M_3$. Other features present in the S^+M_4 mass channel, as a result of dissociation of the ionized clusters, include two isomers of each of the SM_5 and SM_6 clusters.

The red shifted spectrum of the SM_4 cluster, unlike the SM, SM_2, and SM_3 clusters, may indicate a major departure from the structure that allows hydrogen bonding interaction between the OH group of methanol and the styrene π-system. A possible structure may involve a cyclic methanol tetramer placed above the styrene molecular plane. This structure is expected to enhance the dispersion and induction interactions, which typically result in red spectral shifts. The calculated lowest energy structures of the SM_4 cluster, presented and discussed in the companion paper,[31] are consistent with the proposed cyclic methanol tetramer above the styrene plane.

Two geometrical isomers are assigned to the SM_5 cluster, which appear in both the SM_5 and SM_4 mass channels. The first isomer (SM_5-I) has a strong origin at -59 cm^{-1} and possesses two vdW peaks at -41 and -25 cm^{-1} (corresponding to peaks 1 and 2 following the SM_5-I origin in the SM_5 channel in Figure 3). The second isomer (SM_5-II) displays a weak low-energy origin at -119 cm^{-1} followed by a stronger vdW multiplet at -115, -110, -105, and -103 cm^{-1} (corresponding to peaks $1-4$ following the SM_5-II origin in the SM_5 channel in Figure 3). Other weak vdW peaks appear at -108 and -98 cm^{-1} and possess significant intensities in the SM_4 mass channel. The origins of both isomers and their vdW features also appear in the S^+M_4 mass channel as a result of ion fragmentation.

The SM_6 mass channel contains features belonging to both the SM_6 and SM_7 clusters. Two isomers SM_6-I and SM_6-II can be assigned to the SM_6 cluster with origins at -46 and -113 cm^{-1}, respectively. Several weaker features with a long progression are assigned to vdW modes associated with the

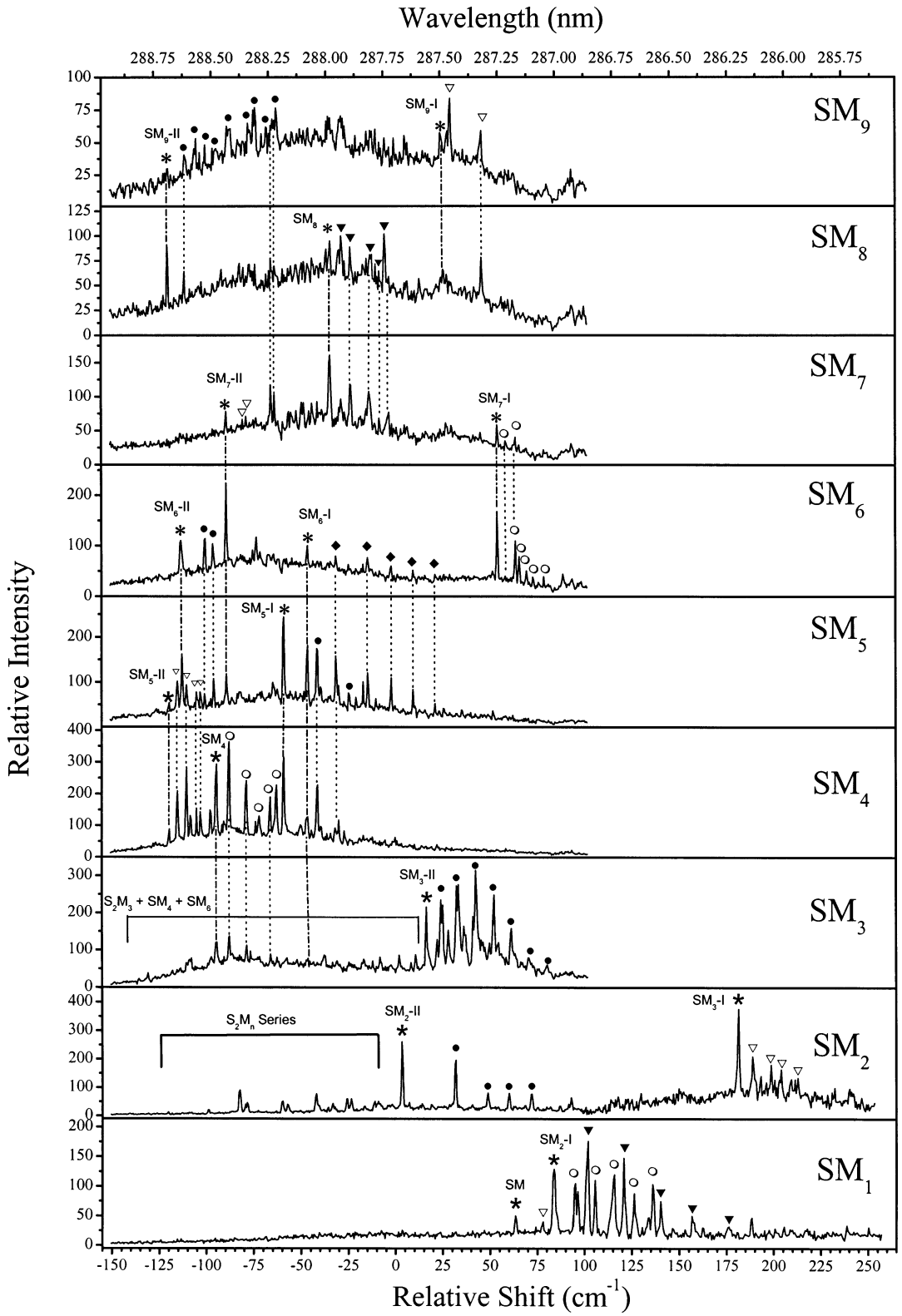

Figure 5. Overall R2PI spectra measured in the styrene (methanol)$_n$ mass channels (SM$_n$) with $n = 9$, relative to the electronic origin band of the $S_1 \leftarrow S_0$ transition of the styrene molecule at 34 758.79 cm^{-1}. The origin of each cluster isomer is marked with an *. The peaks labeled with symbols following each cluster's origin represent vdW bands associated with the cluster origin (see Table 1).

SM_6−I isomer and they appear at −31, −14, −2, 10, and 21 cm^{-1} from the styrene origin (corresponding to peaks 1−5 following the SM_6−I origin in the SM_6 channel in Figure 3). The SM_6−I isomer undergoes extensive fragmentation to both the SM_5 and the SM_4 mass channels following photoionization of the cluster. The fragmentation also proceeds through the associated vdW modes as evident in the SM_4 and SM_5 mass channels. The SM_6−II origin (−113 cm^{-1}) has two vdW peaks at −100 and −96 cm^{-1} and both fragment to the SM_5 mass channel.

D. Spectra of SM$_n$ Clusters, $n = 7-9$. Figure 4 displays the R2PI spectra obtained by monitoring the mass channels corresponding to the SM_7, SM_8, and SM_9 clusters. The SM_7 cluster shows two distinct isomers (SM_7−I and SM_7−II) with

TABLE 1: Spectral Features Observed in the SM$_n$ Mass Channels (S = Styrene, M = Methanol, vdW = van der Waals Mode)

cluster	shift (cm^{-1}) from the 0_0^0 of styrene	obsd mass channel	rel intens	assgnt	shift (cm^{-1}) from cluster's origin
SM	63.4	SM	50	SM origin	0
	78.0	SM	41	vdW	14.6
SM$_2$−I	83.8	SM	128	SM$_2$−I origin	0
	95.2/96.4	SM	104/92	vdW-a	11.4/12.6
	102.2	SM	176	vdW-1	18.4
	105.8	SM	110	vdW-b	22.0
	116.2	SM	120	vdW-c	32.4
	121.1	SM	147	vdW-2	37.3
	126.5	SM	88	vdW-d	42.7
	136.3	SM	103	vdW-e	52.6
	140.6	SM	75	vdW-3	56.8
	157.0	SM	50	vdW-4	73.2
	176.6	SM	32	vdW-5	92.6
SM$_2$−II	3.4	SM$_2$	262	SM$_2$−II origin	0
	32.0	SM$_2$	197	vdW-1	28.6
	48.9	SM$_2$	81	vdW-2	45.5
	60.1	SM$_2$	91	vdW-3	56.7
	72.2	SM$_2$	79	vdW-4	68.8
SM$_3$−I	181.6	SM$_2$	377	SM$_3$−I origin	0
	188.9	SM$_2$	210	vdW-1	7.3
	198.7	SM$_2$	181	vdW-2	17.1
	204.1	SM$_2$	165	vdW-3	22.5
	212.9	SM$_2$	135	vdW-4	31.3
	232.4	SM$_2$	100	VdW-5	50.8
	241.2	SM$_2$	86	VdW-6	59.6
SM$_3$−II	16.5	SM$_3$	216	SM$_3$–II origin	0
	24.2	SM$_3$	235	vdW-1	7.7
	28.1	SM$_3$	153	vdW	11.6
	33.4	SM$_3$	276	vdW-2	16.9
	36.3	SM$_3$	164	vdW	19.8
	42.6	SM$_3$	315	vdW-3	26.1
	52.3	SM$_3$	248	vdW-4	35.8
	61.5	SM$_3$	158	vdW-5	45
	70.2	SM$_3$	79	vdW-6	53.7
	80.4	SM$_3$	60	vdW-7	63.9
SM$_4$	−94.4	SM$_3$	121	SM$_4$ origin	0
	−94.4	SM$_4$	293	SM$_4$ origin	0
	−87.6	SM$_3$	137	vdW-1	6.8
	−87.6	SM$_4$	363	vdW-1	6.8
	−78.5	SM$_3$	112	vdW-2	15.9
	−78.5	SM$_4$	241	vdW-2	15.9
	−71.8	SM$_3$	81	vdW-3	22.6
	−71.8	SM$_4$	130	vdW-3	22.6
	−66.0	SM$_3$	88	vdW-4	28.4
	−66.0	SM$_4$	189	vdW-4	28.4
	−62.6	SM$_3$	81	vdW-5	31.8
	−62.6	SM$_4$	228	vdW-5	31.8
SM$_5$−I	−58.8	SM$_4$	314	SM$_5$−I origin	0
	−58.8	SM$_5$	244	SM$_5$−I origin	0
	−41.4	SM$_3$	66	vdW-1	17.4
	−41.4	SM$_4$	228	vdW-1	17.4
	−41.4	SM$_5$	174	vdW-1	17.4
	−24.6	SM$_3$	67	VdW-2	34.2
	−24.6	SM$_5$	76	vdW-2	34.2
SM$_5$−II	−119.3	SM$_4$	89	SM$_5$−II origin	0
	−119.3	SM$_5$	54	SM$_5$−II origin	0
	−115.5	SM$_3$	47	vdW-1	4.0
	−115.5	SM$_4$	210	vdW-1	4.0
	−115.5	SM$_5$	102	vdW-1	4.0
	−110.2	SM$_3$	64	vdW-2	9.1
	−110.2	SM$_4$	284	vdW-2	9.1
	−110.2	SM$_5$	93	vdW-2	9.1
	−108.3	SM$_4$	131	vdW	11.0
	−104.9	SM$_4$	155	vdW-3	14.4
	−104.9	SM$_5$	78	vdW-3	14.4
	−103.1	SM$_4$	143	vdW-4	16.2
	−103.1	SM$_5$	78	vdW-4	16.2
	−97.7	SM$_4$	148	vdW	21.6
SM$_6$−I	−46.2	SM$_3$	77	(SM$_6$−I) origin	0
	46.2	SM$_4$	127	(SM$_6$−I) origin	0
	46.2	SM$_5$	181	(SM$_6$−I) origin	0
	46.2	SM$_6$	100	(SM$_6$−I) origin	0
	−30.8	SM$_3$	71	vdW-1	15.4
	−30.8	SM$_4$	92	vdW-1	15.4
	−30.8	SM$_5$	157	vdW-1	15.4
	−30.8	SM$_6$	80	vdW-1	15.4
	−14.4	SM$_5$	120	vdW-2	31.8
	−14.4	SM$_6$	77	vdW-2	31.8
	−1.9	SM$_5$	109	vdW-3	44.3
	−1.9	SM$_6$	60	vdW-3	44.3
	9.7	SM$_5$	83	vdW-4	55.9
	9.7	SM$_6$	52	vdW-4	55.9
	21.3	SM$_5$	52	vdW-5	67.5
	21.3	SM$_6$	44	vdW-5	67.5
SM$_6$−II	−112.6	SM$_5$	162	SM$_6$−II origin	0
	−112.6	SM$_6$	110	SM$_6$−II origin	0
	−100.6	SM$_5$	74	vdW-1	12.0
	−100.6	SM$_6$	114	vdW-1	12.0
	−95.8	SM$_5$	107	vdW-2	16.8
	−95.8	SM$_6$	104	vdW-2	16.8
SM$_7$−I	54.2	SM$_6$	168	SM$_7$−I origin	0
	54.2	SM$_7$	58	SM$_7$−I origin	0
	58.6	SM$_6$	41	vdW-1	4.4
	58.6	SM$_7$	35	vdW-1	4.4
	63.9	SM$_6$	110	vdW-2	9.7
	63.9	SM$_7$	41	vdW-2	9.7
	65.9	SM$_6$	79	vdW-3	11.7
	69.8	SM$_6$	50	vdW-4	15.6
	73.1	SM$_6$	38	vdW-5	18.9
	79.0	SM$_6$	39	vdW-6	24.8
SM$_7$−II	−89.1	SM$_5$	118	SM$_7$−II origin	0
	−89.1	SM$_6$	224	SM$_7$−II origin	0
	−89.1	SM$_7$	78	SM$_7$−II origin	0
	−80.4	SM$_6$	81	vdW	8.7
	−80.4	SM$_7$	67	vdW	8.7
	−78.5	SM$_7$	71	vdW-2	10.6
	−73.2	SM$_6$	117	vdW	15.9
SM$_8$	36.1/34.2	SM$_8$	86/95	SM$_8$ origin	
	−34.2	SM$_7$	161	SM$_8$ origin	0
	−28.4	SM$_7$	96	VdW-1	7.7
	−28.4	SM$_8$	100	vdW-1	7.7
	−23.1	SM$_7$	117	VdW-2	13
	−23.1	SM$_8$	89	vdW-2	13
	−13.5	SM$_7$	108	VdW-3	22.6
	−13.5	SM$_8$	81	vdW-3	22.6
	−8.2	SM$_7$	68	VdW-4	27.9
	−8.2	SM$_8$	65	vdW-4	27.9
	−2.84	SM$_7$	77	VdW-5	33.26
SM$_9$−I	24.2/25.7	SM$_8$	66	SM$_9$−I origin	
	24.2	SM$_9$	58	SM$_9$−I origin	0
	29.5	SM$_9$	84	VdW-1	5.3
	46.0	SM$_8$	78	VdW-2	20.3
	46.0	SM$_9$	59	vdW-2	20.3
SM$_9$−II	−120.3	SM$_8$	91	SM$_9$−II origin	0
	−120.3	SM$_9$	30	SM$_9$−II origin	0
	−111.2	SM$_8$	64	VdW-1	9.1
	−111.2	SM$_9$	40	vdW-1	,
	−104.9	SM$_9$	53	vdW-2	15.4
	−100.1	SM$_9$	48	vdW-3	20.2
	−94.4	SM$_9$	45	vdW-4	25.9
	−86.7	SM$_9$	61	vdW-5	33.6
	−77.5	SM$_9$	65	vdW-6	42.8
	−73.7	SM$_9$	77	vdW-7	46.6
	−67.9	SM$_9$	61	vdW-8	52.4
	−62.6	SM$_9$	77	vdW-9	57.7

origins at +54 and −89 cm^{-1}, respectively. Both clusters fragment efficiently upon photoionization into the SM$_6$ mass channel. The SM$_7$−I isomer exhibits a small vdW multiplet at 64, 66, 70, 73, and 79 cm^{-1} with greater intensity in the SM$_6$ mass channel due to ion fragmentation (corresponding to peaks 2−6 following the SM$_7$−I origin in the SM$_6$ channel in Figure 3). The second isomer SM$_7$−II shows small vdW peaks at −80/−79, −75, and −73 cm^{-1}. The remaining features in the SM$_7$ mass channel belong to the SM$_8$ and SM$_9$ clusters. The SM$_8$ cluster origin appears in the SM$_8$ mass channel at −36/−

34 cm^{-1}. A vdW progression associated with the SM_8 cluster appears at −28, −23, −14, −8, and −3 cm^{-1}, corresponding to peaks 1−5, respectively, following the SM_8 origin in the SM_8 channel in Figure 4. The SM_8 cluster has a doublet origin and shows strong fragmentation into the SM_7 mass channel through the vdW modes which appear at −34, −28, −23, −14, −8, and −5 cm^{-1}. The other features in the SM_8 mass channel can be assigned to the SM_9 cluster, as shown in Figure 4. On the basis of the comparison of the spectral features in the SM_8 and SM_9 mass channels, we assign the peak at −120 cm^{-1} to one isomer of the SM_9 cluster (SM_9−II). This isomer shows several vdW peaks at −111, −105, −100, −94, −87, −78, −74, −68, and −63 cm^{-1} corresponding to peaks 1−9, respectively, following the SM_9−II origin in the SM_9 channel in Figure 4. Another origin in the SM_9 mass channel at +24 cm^{-1} followed by a doublet at +29/30 cm^{-1} and a vdW peak at +46 cm^{-1} is assigned to a second isomer of the SM_9 cluster (SM_9−I). It is interesting to note that all the assigned isomers of the SM_n clusters with $n = 4-9$ exhibit red spectral shifts, relative to the styrene origin, except for the SM_7−I and SM_9−I isomers, which display blue shifts. Figure 5 exhibits the overall R2PI spectra recorded in the SM_n mass channels with $n = 1-9$, displayed relative to the 0_0^0 origin of styrene. The relative frequencies and tentative assignments of the SM_n cluster isomers are listed in Table 1.

E. Spectral Shifts. The spectral shifts relative to the 0_0^0 origin of the isolated styrene molecule imposed by methanol clusters provide information on the nature of the intermolecular interactions within the binary clusters. Spectral shifts are due to different cluster binding energies in the ground and excited states. A red shift implies that the excited state is more tightly bound than the ground state, and a blue shift is associated with stronger interaction in the ground state. A red shift is usually observed in clusters where the dispersion energy is dominant due to the increase in the molecular polarizability in the excited state relative to the ground state.[45,46] For example, ring−ring interactions result in red shifts because dispersive forces are stronger for the more delocalized excited states, as in benzene and other aromatic clusters.[47,48] On the other hand, hydrogen bonding to the π-system results in a blue shift, which tends to increase with increasing the H-bond donating capacity of the solvent molecules.[9]

In contrast to benzene, few studies of clusters containing styrene have been reported.[41,49−59] Clusters of styrene with Ar, N_2, CO_2, NH_3, and trimethylamine were studied by laser-induced fluorescence (LIF) and REMPI.[44,52−56] The origin bands of these clusters are shifted by −31, −25.5, +51, +52, and −24 cm^{-1} relative to the 0_0^0 band of the bare styrene molecule. The spectra of the styrene−TMA 1:1 cluster were assigned to two isomeric forms, both capable of forming a charge-transfer complex upon excitation to the locally excited state.[52,53] We recently reported the REMPI spectra of styrene $(water)_n$ clusters, SW_n, with $n = 1-2$, which indicate that the origin of the SW complex is blue shifted by −22 cm^{-1} relative to the 0_0^0 band of the bare styrene molecule.[57]

In the case of methanol clusters, the binding energy is mainly due to hydrogen bonding. Monte Carlo, molecular dynamics, density functional, and ab initio calculations have shown that the intermolecular interactions in small methanol clusters ($n = 4-9$) are dominated by configurations in which hydrogen-bonded chains are formed with cyclic structures starting at $n = 3$.[58−63] If it is assumed that the styrene molecule does not significantly affect hydrogen bonding in methanol clusters, then

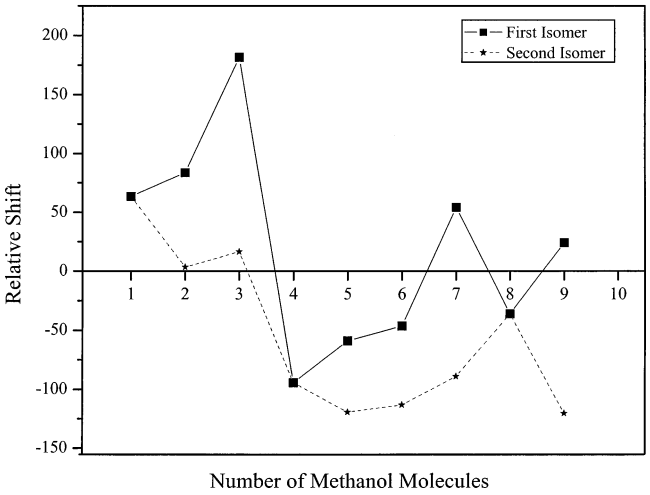

Figure 6. Spectral shifts of the origins of the SM_n clusters, relative to the 0_0^0 band of styrene, as a function of n.

shifts of the electronic origin of SM_n clusters can be related to the styrene ↔ (methanol subcluster) interaction.

Figure 6 displays the observed spectral shifts of the SM_n cluster origins, relative to the 0_0^0 transition of styrene, as a function of n. The observed pattern reveals some interesting correlation with the proposed structures of the clusters. Figures 5 and 6 show that the first isomers of SM_n ($n = 1-3$) exhibit successively greater increases in blue shift, which reaches a maximum of 182 cm^{-1} for the SM_3−I isomer. The shifts of these isomers are consistent with H-bonding to the π-system of styrene. The SM_2−II and SM_3−II isomers exhibit smaller blue shifts, which may reflect more dispersive interactions, suggesting structures with no directional hydrogen bonding to the π-system of styrene. The calculated structures of these isomers are presented in the companion paper.[31]

The spectral shift reverses direction in the single isomer observed for SM_4. The successive addition of methanol molecules to the SM complex leads to a stable cyclic methanol tetramer in SM_4 that is unable to H-bond to the styrene π-system, consistent with the observed red shift.

The two isomers assigned to each of the SM_5 and SM_6 clusters may contain cyclic methanol subclusters. Similarly, the two SM_7 cluster isomers could have cyclic five- or six-member rings with the other molecule(s) as ring branches. The single isomer assigned to the SM_8 cluster could involve a bicyclic methanol ring structure. Also, the two SM_9 isomers could represent a larger bicyclic ring containing nine methanol molecules, and a bicyclic eight-member ring on one side of styrene and a free methanol molecule on the other side of the styrene plane. Interestingly, the addition of the red shift of −36 cm^{-1} imposed by the SM_8 cluster and the blue shift of +63 cm^{-1} of the SM cluster results in a +27 cm^{-1} shift, which is similar to the observed shift of the SM_9−I isomer. This may suggest that the SM_9−I isomer consists of a M_8 subcluster on one side of styrene and a single methanol molecule on the other. The arrangement of the methanol molecules with respect to the styrene plane has been investigated using pair potentials, and the results are presented and discussed in the companion paper.[31]

F. Fragmentation of the Ionized Clusters. The ionization potential of the styrene molecule is 68 267 cm^{-1}.[64] Because the 0_0^0 transition is located at 34 758.79 cm^{-1}, two photons resonant with the origin transition suffice to ionize styrene in a one-color REMPI experiments. The ionic state of the styrene molecule in the SM_n cluster is prepared according to the Franck−Condon distribution, whereas the rest of the cluster

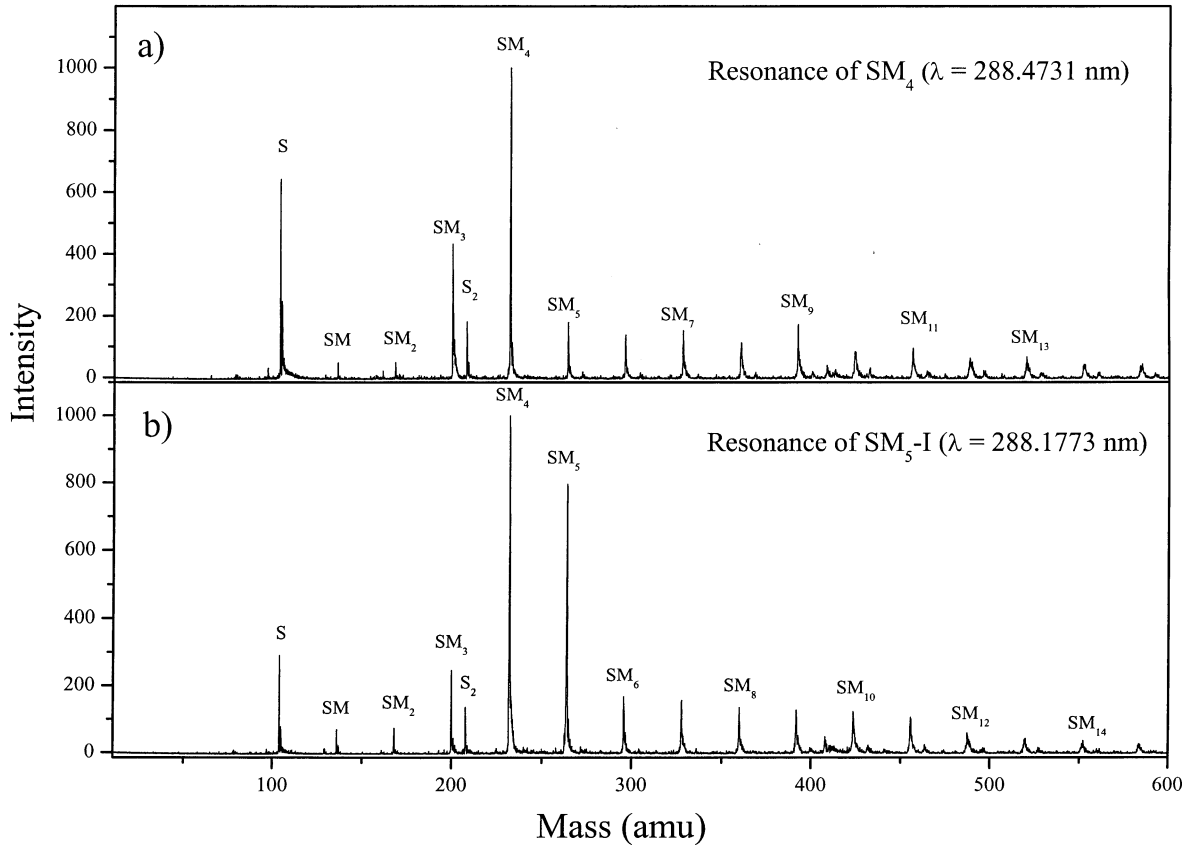

Figure 7. R2PI mass spectra of the styrene−methanol (SM$_n$) cluster beam obtained at the resonance ionizations assigned to the origins of (a) SM$_4$ and (b) SM$_5$−I clusters.

relaxes structurally in a time-dependent manner about the styrene ion. This relaxation releases energy and thus lowers the cluster ionization threshold relative to that of the isolated styrene molecule, and the additional energy imparted to the S^+M_n cluster ion promotes fragmentation via solvent evaporation from the cluster. However, because a large fraction of the energy usually goes to the electron, some cluster ions are formed with little internal energy and may not dissociate while in the acceleration zone of the TOF (typically 1−2 μs in these experiments). If the time scales for the post-ionization fragmentation processes [$S^+M_n \rightarrow S^+M_{n-m}$] are faster than the time of acceleration in the mass spectrometer, then the resonant intensity of cluster n will contribute to the observed intensity of cluster $n-m$. These time scales will in general depend on the cluster's internal energy prior to excitation, the final energy state produced by ionization, and the time scale of energy relaxation into the intermolecular modes.

Fragmentation probabilities are measured by comparing the absolute integrated intensities I_n at various mass channels (parent I_n and daughters I_{n-1}, I_{n-2}, etc.) at the laser wavelength of a specific spectral resonance and normalizing to the sum over $I_n + I_{n-1} +$ .... The results expressed as a percent of the parent ion intensity are shown in Table 2.

The relatively efficient fragmentation observed for the S^+M complex following photoionization is a direct consequence of the π-hydrogen-bonded geometry of the neutral complex. The structural change in going from the π-hydrogen-bonding geometry in the neutral species to the predominantly ion−dipole interaction in the ionized species involves a great strain, which leads to efficient fragmentation. However, the fragmentation of the S^+M complex is significantly less than that of the B^+M complex (where almost 100% fragmentation was observed). This

TABLE 2: Fragmentations Probabilities of the SM$_n$ Cluster Ions

fragmentation channel	parent, shift (cm^{-1})	%
SM → S	63.4	65
SM$_2$−I → SM	83.8	96
SM$_2$−II → SM	3.4	4
SM$_3$−I → SM$_2$	181.6	82
SM$_3$−II → SM$_2$	16.5	2
SM$_4$ → SM$_3$	−94.4	20
SM$_5$−I → SM$_4$	−58.8	55
SM$_5$−II → SM$_4$	−119.3	67
SM$_6$−I → SM$_5$	−46.2	48
SM$_6$−II → SM$_5$	−113.1	63
SM$_7$−I → SM$_6$	54.2	81
SM$_7$−II → SM$_6$	−89.1	61
SM$_7$−II → SM$_5$	−89.1	26
SM$_8$ → SM$_7$	−36.1	11
SM$_9$−I → SM$_8$	24.2	27
SM$_9$−II → SM$_8$	−120.3	74

is consistent with the methanol interacting with both the ethylene double bond and the aromatic ring.

Figure 7 displays examples of the mass spectra obtained at some selected resonance features assigned to the SM$_n$ cluster origins. In the two examples displayed in Figure 7, the S^+M_4 and S^+M_5−I clusters show little fragmentation following photoionization, and the mass peaks corresponding to the parent resonance cluster show enhanced intensity. However, when fast ion fragmentation is predominant, significant intensity of the SM$_{n-1}$ ions are observed following the resonant ionization of the SM$_n$ clusters. This is clearly observed in the SM$_2$−I, SM$_3$−I and SM$_7$−I cluster isomers. The small fragmentation probability of the SM$_4$ cluster ion supports the assumption of a ring structure of the methanol tetramer placed above the plane of the styrene molecule. Further evidence for this proposed structure will be

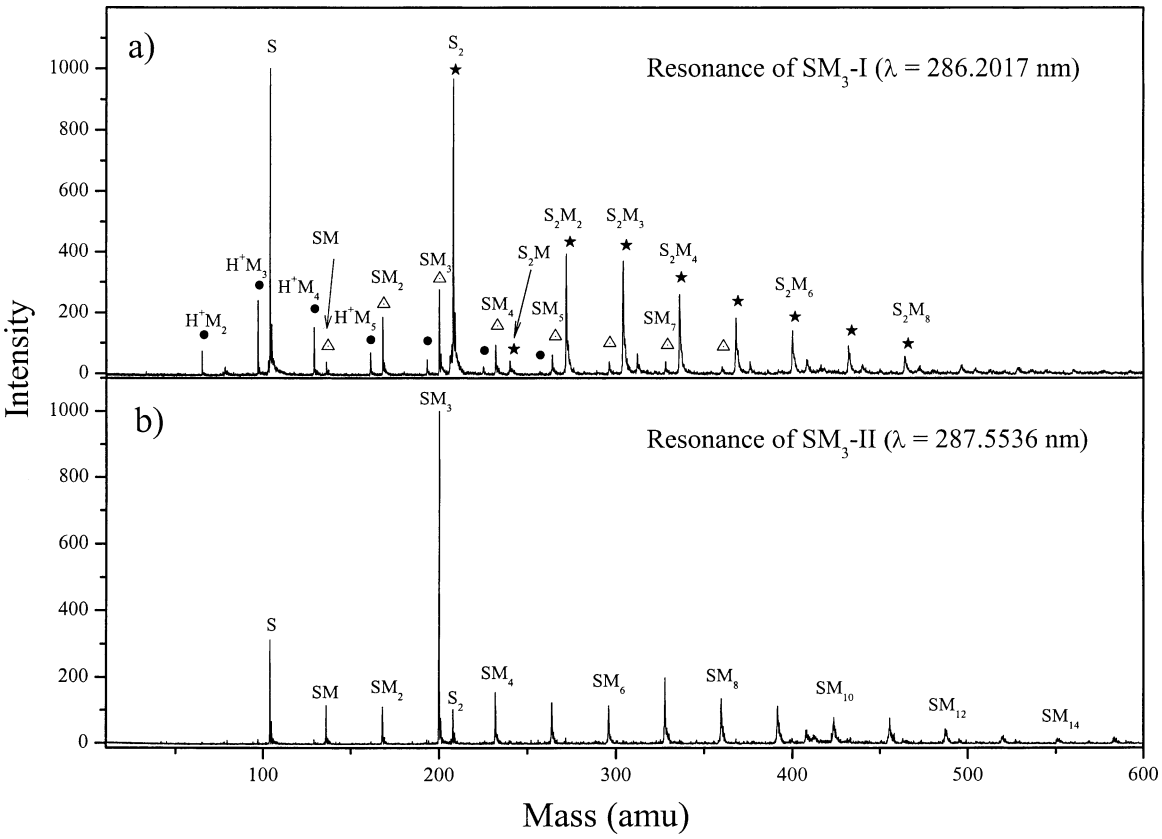

Figure 8. R2PI mass spectra of the styrene−methanol (SM_n) cluster beam obtained at the resonance ionizations assigned to the origins of (a) SM_3−I and (b) SM_3−II clusters. The SM_n series is labeled as △. Note the correlation between the generations of the protonated methanol clusters H^+M_n (labeled as ●) and the styrene dimer series S_2M_n (labeled as ★) as shown in (a).

provided by the minimum energy structures presented in the companion paper.[31]

G. Intracluster Reactions Following Photoionization. Mass spectra of the SM_n clusters obtained at selected resonance ionization energies reveal the generation of protonated methanol clusters H^+M_n starting at $n \geq 2$. Because pure methanol clusters (in the absence of styrene) could not be ionized with the same laser power used in the R2PI experiments, the origin of the protonated clusters must be attributed to the SM_n clusters. The H^+M_n clusters could be produced by either dissociative electron transfer (EDT) or dissociative proton transfer (DPT), or a combination of both mechanisms. The small intensity of the H^+M_n ions (due to the necessity of low laser power to stay within the two photon process) prevented correlation of their spectral features with those of the parent SM_n clusters and the unambiguous determination the origin of the protonated methanol clusters.

Figure 8 displays the mass spectra obtained at wavelengths corresponding to the assigned SM_3−I and SM_3−II cluster origins. It is interesting to note that the protonated methanol clusters are formed exclusively at the resonance of the SM_3−I isomer (286.202 nm) and not at the SM_3−II resonance. However, it should be noted that at this wavelength the mass spectrum contains significant contributions from the styrene dimer ($S_2^{\bullet+}$) and the $S_2M_n^+$ series. The styrene dimer cation has been a subject of several studies that have established it to be covalently bonded ($C_{16}H_{16}^{\bullet+}$) and probably cyclic in structure.[25,26,65−67] The correlation between the generation of the $S_2M_n^+$ series and the protonated methanol clusters suggests that DPT takes place from the styrene dimer cation $C_{16}H_{16}^{\bullet+}$ to the methanol subcluster M_n within the $S_2M_n^+$ cluster to generate the H^+M_n species, as shown in eq 1. At lower laser power, the

$$C_{16}H_{16}^{+}(CH_3OH)_n \rightarrow H^+(CH_3OH)_n + C_{16}H_{15}^{\bullet} \quad n \geq 3 \quad (1)$$

protonated methanol clusters are generated starting at $n = 3$. This suggests that the protonated methanol dimer is produced by evaporation from larger H^+M_n clusters with $n \geq 3$ as shown in eq 2.

$$H^+(CH_3OH)_n \rightarrow H^+(CH_3OH)_{n-1} + CH_3OH \quad (2)$$

The proposed mechanism involves structural changes following the ionization of the styrene dimer resulting in the formation of a covalent bonded styrene dimer cation ($C_{16}H_{16}^{\bullet+}$) solvated by methanol molecules in the cluster. DPT between $C_{16}H_{16}^{\bullet+}$ and methanol subcluster then results in the generation of protonated methanol clusters $[H^+(CH_3OH)_n]$ and the $C_{16}H_{15}^{\bullet}$ radical. It should be noted the DPT channel becomes exothermic in the $S_2M_3^+$ cluster if the proton affinity (PA) of $C_{16}H_{15}^{\bullet}$ $[C_{16}H_{16}^{\bullet+} \rightarrow C_{16}H_{15}^{\bullet} + H^+]$ is less than that of the methanol trimer $[H^+M_3 \rightarrow M_3 + H^+]$. On the basis of the estimation of the PA of M_3 as 224 kcal/mol,[68] the upper limit of the PA of the styrene dimer radical ($C_{16}H_{15}^{\bullet}$) can be estimated as ≥224 kcal/mol.

The DPT mechanism suggested for the generation of the protonated methanol clusters is consistent with our recent study of the styrene/water binary clusters, where isotopic experiments involving D_2O have revealed that the protonated water clusters $H^+(H_2O)_n$ are produced via a DPT mechanism involving the styrene dimer series $[C_{16}H_{16}^{+}(D_2O)_n]$ with $n \geq 3$.[69]

The observed intracluster DPT reactions in $S_2M_n^+$ series are consistent with the detrimental effect of methanol on the bulk cationic polymerization of styrene. For example, it is well established that radiation-induced polymerization of styrene

proceeds via a cationic mechanism in pure, dry bulk styrene.[26−28,70] The presence of a small amount of methanol suppresses the cationic polymerization and enhances both the dimerization and the radical polymerization. It has been shown that methanol reacts with the dimer radical cation and converts it to a neutral radical that initiates the radical polymerization.[27] This is exactly the result obtained in the present work via the DPT mechanism within the $S_2M_n^+$ clusters. The similarity between the cluster and the bulk phase results provides strong evidence for the validity of the cluster approach in elucidating the mechanisms of initiation, propagation and inhibition of cationic polymerization.

IV. Summary and Conclusions

In the present work, well-resolved R2PI spectra of styrene−methanol clusters have been reported. The spectra reveal a rapid increase in complexity with the number of methanol molecules in the cluster, associated with vdW modes and isomeric forms. Although only single cluster origins are found for the SM, SM_4, and SM_8 clusters, two distinct isomers are identified for each of the SM_n clusters with $n = 2$, 3, 5−7, and 9. The progressive addition of methanol molecules to the SM complex leads to the formation of stable cyclic methanol subclusters within the SM_4 and SM_8 clusters. The spectral shifts in the cluster origins reflect the nature of the intermolecular interactions within the binary clusters. Blue shifts are observed for the SM, SM_2, and SM_3 clusters consistent with hydrogen bonding interactions between the OH groups and the styrene π-system. A remarkable switch in the spectral shift from blue to red is observed at the SM_4 cluster consistent with the ring structure of the methanol tetramer. Evidence is provided for intracluster dissociative proton-transfer reactions within the $S_2M_n^+$ clusters with $n \geq 3$ to generate protonated methanol clusters. It is proposed that the interaction of the methanol molecules with the olefin center of styrene promotes the proton transfer from the styrene dimer to the hydrogen-bonded methanol cluster. These reactions may explain the strong inhibition effects exerted by small concentrations of methanol on the cationic polymerization of styrene.

Acknowledgment. We gratefully acknowledge financial support from NSF Grant No. CHE 9816536.

References and Notes

(1) Stone, A. J. *The Theory of Intermolecular Forces*; Clarendon: Oxford, U.K., 1996.
(2) Israelachvili, J. N. *Intermolecular and Surface Forces*; Academic Press: London, 1997.
(3) Hobza, P.; Zahradanik, R. *Intermolecular Complexes*; Academia: Prague, 1988.
(4) Weber, A. *Structure and Dynamics of Weakly Bound Complexes*; NATO-ASI: Washington DC, 1988.
(5) Bernstein, E. R. *Atomic and Molecular Clusters*; Elsevier: Amsterdam, 1990.
(6) Shang, Q. Y.; Bernstein, E. R. *Chem. Rev.* **1994**, *94*, 2015.
(7) Castleman, A. W., Jr.; Wei, S. *Annu. Rev. Phys. Chem.* **1994**, *45*, 685.
(8) Castleman, A. W., Jr.; Bowen, K., Jr. *J. Phys. Chem.* **1996**, *100*, 12911.
(9) Zwier, T. S. *Annu. Rev. Phys. Chem.* **1996**, *47*, 205.
(10) Gotch, A. J.; Zwier, T. S. *J. Chem. Phys.* **1990**, *93*, 6977.
(11) Gord, J. R.; Garrett, A. W.; Bandy, R. E.; Zwier, T. S. *Chem. Phys. Lett.* **1990**, *171*, 443.
(12) Gotch, A. J.; Garrett, A. W.; Severance, D. L.; Zwier, T. S. *Chem. Phys. Lett.* **1991**, *178*, 121.
(13) Gotch, A. J.; Zwier, T. S. *J. Chem. Phys.* **1991**, *96*, 3388.
(14) Garrett, A. W.; Severance, D. L.; Zwier, T. S. *J. Chem. Phys.* **1992**, *96*, 7245.
(15) Pribble, R. N.; Zwier, T. S. *Science* **1994**, *265*, 75.
(16) Gruenloh, C. J.; Carney, J. R.; Arrington, C. A.; Zwier, T. S.; Fredericks, S. Y.; Jordan, K. D. *Science* **1997**, *276*, 1678
(17) Germanenko, I. N.; El-Shall, M. S. *J. Phys. Chem. A* **1999**, *103*, 5847.
(18) Daly, G. M.; Wright, D.; El-Shall, M. S. *Chem. Phys. Lett.* **2000**, *331*, 47.
(19) El-Shall, M. S.; Daly, G. M.; Wright, D. J. *Chem. Phys.* **2002**, *116*, 10253.
(20) Gruenloh, C. J.; Carney, J. R.; Hagemeister, F. C.; Arrington, C. A.; Zwier, T. S.; Fredericks, S. Y.; Wood, J. T., III.; Jordan, K. D. *J. Chem. Phys.* **1998**, *109*, 6601.
(21) Carmey, J. R.; Hagemeister, F. C.; Zwier, T. S. *J. Chem. Phys.* **1998**, *108*, 3379.
(22) Tanford, C. *The Hydrophobic Effect: Formation of Micelles and Biological Membranes*; Wiley: New York, 1980.
(23) Privalov, P.; Gill, S. S. J. *Adv. Protein Chem.* **1988**, *40*, 191.
(24) Jeffrey, J. A.; Sanger, W. *Hydrogen Bonding in Biological Structures*; Springer−Verlag: Berlin 1991.
(25) Kennedy, J. P.; Marechal, E. *Carbocationic Polymerization*; John Wiley & Sons: New York, 1982.
(26) Odian, G. *Principles of Polymerization*; McGraw-Hill: New York, 1970.
(27) Silverman, J.; Tagawa, S.; Kobayashi, H.; Katsumura, Y.; Washio, M.; Tabata, Y. *Radiat. Phys. Chem.* **1983**, *22*, 1039.
(28) Tagawa, S.; Schnabel, W. *Chem. Phys. Lett.* **1980**, *75*, 120.
(29) Narten, A. H.; Habenschuss, A. *J. Chem. Phys.* **1984**, *80*, 3387.
(30) Steylter, D. C.; Dore, J. C.; Montague, D. C. *J. Non-Cryst. Solids* **1985**, *74*, 303.
(31) El-Shall, M. S.; Wright, D.; Ibrahim, Y.; Mahmoud, H. *J. Phys. Chem. A* **2003**, *107*, 5933.
(32) Hollas, J. M.; Khalilipour, E.; Thakur, S. N. *J. Mol. Spectrosc.* **1978**, *73*, 240.
(33) Hollas, J. M.; Musa, H.; Ridley, T.; Turner, P. H.; Weisenberger, K. H. *J. Mol. Spectrosc.* **1982**, *94*, 437.
(34) Syage, J. A.; Al Adel, F.; Zewail, A. H. *Chem. Phys. Lett.* **1983**, *103*, 15.
(35) Seeman, J. I.; Grassian, V. H.; Bernstein, E. R. *J. Am. Chem. Soc.* **1988**, *110*, 8542.
(36) Caminati, W.; Vogelsanger, B.; Bauder, A. *J. Mol. Spectrosc.* **1988**, *128*, 384.
(37) Bock, C. W.; Trachtman, M.; George, P. *Chem. Phys.* **1985**, *93*, 431.
(38) Hamley, R. J.; Dinur, U.; Vaida, V.; Karplus, M. *J. Am. Chem. Soc.* **1985**, *107*, 836.
(39) Gordon, M. H.; Pople, J. A. *J. Phys. Chem.* **1993**, *97*, 1147.
(40) Hargiti, R.; Szalay, P. G.; Pongor, G.; Foragasi, G. *J. Mol. Struct. (THEOCHEM)* **1994**, *306*, 293.
(41) Ziberg, S.; Haas, Y. *J. Chem. Phys.* **1995**, *103*, 20.
(42) Ribblett, J. W.; Borst, D. R.; Pratt, D. W. *J. Chem. Phys.* **1999**, *111*, 8454.
(43) Chia, L.; Goodman, L.; Philis, J. G. *J. Chem. Phys.* **1983**, *79*, 593.
(44) Kendler, S.; Haas, Y. *Chem. Phys. Lett.* **1995**, *236*, 324.
(45) Longuet-Higgins, H. C.; Pople, J. A. *J. Chem. Phys.* **1957**, *27*, 192.
(46) Shalev, E.; Ben-Horin, N.; Jortner, J. *J. Chem. Phys.* **1991**, *94*, 7757. Shalev, E.; Ben-Horin, N.; Even, U.; Jortner, J. *J. Chem. Phys.* **1991**, *95*, 3147.
(47) Easter, D. C.; El-Shall, M. S.; Hahn, M. Y.; Whetten, R. L. *Chem. Phys. Lett.* **1989**, *157*, 277.
(48) Bach, A.; Leutwyler, S. *Chem. Phys. Lett.* **1999**, *299*, 381.
(49) Dyke, J. M.; Ozeki, H.; Takahashi, M.; Cookett, M. C. R.; Kimura, K. *J. Chem. Phys.* **1992**, *97*, 8926.
(50) Consalvo, D.; van der Avoird, A.; Piccirillo, S.; Coreno, M.; Giardini-Guidoni, A.; Mele, A.; Snels, M. *J. Chem. Phys.* **1993**, *99*, 8398.
(51) Piccirillo, S.; Consalvo, D.; Coreno, M.; Giardini-Guidoni, A.; Douin, S.; Parneix, P.; Brechignac, P. *Chem. Phys.* **1994**, *187*, 97.
(52) Zingher, E.; Kenler, S.; Haas, Y. *Chem. Phys. Lett.* **1996**, *254*, 213.
(53) Kendler, S.; Haas, Y. *J. Phys. Chem. A* **1997**, *101*, 2578.
(54) Douin, S.; Piccirillo, S.; Brechignac, P. *Chem. Phys. Lett.* **199**7, *273*, 389.
(55) Foltin, M.; Stueber, G. J.; Bernstein, E. R. *J. Chem. Phys.* **1998**, *109*, 4342.
(56) Zensen, T. A.; Jarski, P.; Eaton, J. G. *Chem. Phys. Lett.* **2000**, *326*, 389.
(57) Mahmoud, H.; Germanenko, I. N.; Ibrahim, Y.; El-Shall, M. S. *Chem. Phys. Lett.* **2002**, *356*, 91.
(58) Sim, F.; St-Amant, A.; Papai, I.; Salahub, D. R. *J. Am. Chem. Soc.* **1992**, *114*, 4391.
(59) Wright, D.; El-Shall, M. S. *J. Chem. Phys.* **1996**, *105*, 11199.
(60) Mo, O.; Yanez, M.; Elguero, J. *J. Chem. Phys.* **1997**, *107*, 3592.
(61) Buck, U.; Siebers, J. G.; Wheatley, R. J. *J. Chem. Phys.* **1988**, *108*, 20.

(62) Zakharov, V. V.; Brodskya, E. N.; Laaksonen, A. *J. Chem. Phys.* **1998**, *109*, 9487.

(63) Hgemeister, F. C.; Gruenloh, C. J.; Zwier, T. S. *J. Phys. Chem. A* **1998**, *102*, 82.

(64) Dyke, J. M.; Ozeki, H.; Takahashi, M.; Cockett, M. C. R.; Kimura, K. *J. Chem. Phys.* **1992**, *97*, 8926.

(65) Groenewold, G. S.; Chess, E. K.; Gross, M. L. *J. Am. Chem. Soc.* **1984**, *106*, 539.

(66) Pithawalla, Y. B.; Gao, J.; Yu, Z.; El-Shall, M. S. *Macromolecules* **1996**, *29*, 8558.

(67) El-Shall, M. S.; Yu, Z. *J. Am. Chem. Soc.* **1996**, *118*, 13058.

(68) *Gas phas Ion and Neutral Thermochemistry*; Lias, S. G., Barmess, J. E., Liebman, J. F., Holmes, J. L., Levin, R. D., Mallard, W. G., Eds.; Journal of Physical and Chemical Reference Data; American Chemical Society: Washington, DC, 1988; Vol. 17, p 231.

(69) Mahmoud, H.; Ibrahim, Y.; El-Shall, M. S. Manuscript in preparation.

(70) Gotoh, T.; Yamamoto, M.; Nishijima, Y. *J. Polym. Sci A-1* **1981**, *19*, 1047. Machi, S.; Silverman, J.; Metz, D. J. *J. Phys. Chem.* **1972**, *76*, 930. Tagawa, S.; Schnabel, W. *Makromol. Chem. Rapid. Commun.* **1980**, *1*, 345.